

HOSTED BY



ELSEVIER

Contents lists available at ScienceDirect

Engineering Science and Technology, an International Journal

journal homepage: www.elsevier.com/locate/jestch

Full Length Article

Prediction and optimization of surface roughness in thermal drilling using integrated ANFIS and GA approach

R. Kumar^{a,*}, N. Rajesh Jesudoss Hynes^b^a Department of Mechanical Engineering, Vels Institute of Science, Technology & Advanced Studies, Pallavaram, Chennai, Tamil Nadu 600117, India^b Department of Mechanical Engineering, Mepco Schlenk Engineering College, Sivakasi, Tamil Nadu 626005, India

ARTICLE INFO

Article history:

Received 6 September 2018

Revised 2 April 2019

Accepted 23 April 2019

Available online xxx

Keywords:

Thermal drilling

Surface roughness

Adaptive network-based fuzzy inference system

Genetic algorithm

Genetic algorithm

ABSTRACT

In the recent decade, thermal drilling is becoming popular in aerospace and automobile industries because of its unique advantages over conventional twist drilling process. Surface finish of the thermally drilled hole along with its bushing, is a major concern in all crucial applications and it is worthy of investigation. In the present study, the surface roughness of the thermally drilled hole on galvanized steel is predicted and then optimization is carried out, employing an integrated adaptive network-based fuzzy inference system (ANFIS) and genetic algorithm (GA) approach. Experimentation is based on Taguchi L27 orthogonal array and significant parameters such as spindle speed, angle of tool and workpiece thickness are varied in different levels keeping feed rate as constant. Using the experimental results, an ANFIS model is developed for prediction of surface roughness. An objective function is then formulated on minimization of surface roughness with the help of predicted results of the ANFIS model. Then this objective function was imported into GA toolbox of MATLAB software to optimum values of surface roughness of thermally drilled hole. High degree of closeness is observed between the experimental and predicted results. It is also found that the spindle speed and angle of tool play a significant role on the surface roughness of drilled holes in galvanized steel.

© 2019 Karabuk University. Publishing services by Elsevier B.V. This is an open access article under the CC BY-NC-ND license (<http://creativecommons.org/licenses/by-nc-nd/4.0/>).

1. Introduction

Thermal drilling is a non-conventional hole making process in which frictional heat produced between the drill and workpiece is utilized to produce a hole in the sheet metal or thin-walled component at a single processing step and it eventually forms a bush or sleeve-like shape at the backside of the workpiece without generating chip material [1]. The portion of the bushing can be used for forming threads and offers secure support to join the sheet metal components [2]. The length of the bushing is approximately 2 to 3 times the original sheet thickness [3]. This process is also named the friction drilling [4], flow drilling [5], and friction stir drilling [6].

The difficulties in the traditional drilling process such as the production of more amount of unwanted chip, adhesion of hot chip with the twist drill and the possibility of making threads only on the workpiece with considerable thickness [7]. Besides, joining of any two sheet metals by traditional approach needs some methodologies such as inserting of threaded rivets or welding of a nut at

the back of sheet metal. The discrepancy in the strength of such joints leads to difficulty in handling of heavy loads. Above mentioned problems could be rectified by the implementation of thermal drilling process for drilling of sheet metal and it has remarkable applications in the manufacturing industries.

The thermal drilling process is completed with the subsequent stages. In the first stage, the drilling tooltip makes in contact with the surface of the workpiece and accordingly, it starts to pierces the workpiece. In the second stage, due to the frictional contact at the interface, a high temperature is produced which leads to achieve a smooth piercing. Then in the third stage, softening of workpiece takes place and then drilling tool pierces downward to form the bush like shape which surrounds the drilled hole. At the final stage, the drilling tool moves upward and attains the starting position.

Some investigators have reported the experimental and numerical simulation of thermal drilling process which is discussed below.

Miller et al. [8] proposed an investigation of tool wear in the thermal drilling of 1.5 mm thickness AISI 1015 carbon steel. It was found that the characteristic of tool wear by weight loss measurement and also changes in its shape were measured by coordinate measuring machine. Results were confirmed that the carbide

* Corresponding author.

E-mail address: mepcokumar@gmail.com (R. Kumar).

Peer review under responsibility of Karabuk University.

thermal drill was durable with minimum tool wear even after 11,000 holes and also by the microstructural investigation severe abrasive grooves were noticed on the tip of the drill.

Ozler et al. [9] studied the thermal drilling on square shaped cross-sectional AISI 1010 steel tube with a thickness of 2 mm by using a tungsten carbide tool. They have examined the responses such as washer geometry, petal geometry and bushing length under the different parametric settings. It was reported that at a high spindle speed, the improvement of bushing length was noticed but at a high feed rate, the distortion of bushing length has occurred.

Miller et al. [10] investigated the thermal drilling experiments on AISI 1020 steel sheet and finite element simulation of the process using ANSYS 7.0 software under the processing conditions of constant feed rate and spindle speed of the thermal drill. Also, the mathematical models for torque and axial force were occurred based on the criteria of surface contact in between the workpiece and drill. It was reported that the good relationship is exhibited between the results of experimental and simulation.

Bilgin et al. [11] developed a 3D numerical model for thermal drilling on austenitic stainless steel and computed the torque and axial force occurred. DEFORM-3D software tool was used for finite element analysis of this process. It has been reported that the values of torque and axial force decreased and the temperature of workpiece increased with an increase in spindle speed.

Some optimization methods have been proposed by investigators to optimize the process parameters in the thermal drilling process. Table 1 lists the optimization of thermal drilling process using different methods. Pantawane et al. [12] explored that the application of tungsten carbide tool on AISI 1015 steel and examined the effects of process parameters such as feed rate, workpiece thickness to tool diameter ratio, and spindle speed on the response factors of surface roughness, axial force, and torque. Optimal process parameters were obtained by Taguchi method and significance of each parameter was analyzed by Analysis of Variance (ANOVA) method.

Ku et al. [13] optimized that the thermal drilling process parameter using the Taguchi method, during drilling of 2 mm thickness SUS 304 stainless steel. It was studied that the effect of process

parameters of thermal drilling on the output characteristics such as surface roughness and bushing length. ANOVA was used to examine the significance of spindle speed, friction contact area ratio, feed rate, and friction angle on the responses considered for this work. They reported that the spindle speed and friction angle were the important parameters which affect the roughness. Friction contact area ratio was identified as an only significant factor which affects the bushing length.

Chow et al. [14] studied that the behaviour of sintered carbide thermal drill for drilling of AISI 304 steel and investigation was conducted based on Taguchi L18 orthogonal array. Surface roughness for all thermal drilled holes was measured and studied the optimal conditions of input process parameters such as drilling speed, friction contact area ratio, friction angle and feed rate to achieve least surface roughness. Microstructure investigation was employed to demonstrate the surface finishing occurred during the process. Also, the micro-hardness test was revealed that the higher hardness with fine grain structure was found in the surrounding area of the drilled hole.

Krishna et al. [15] conducted the thermal drilling experiments based on Taguchi L8 orthogonal array on AA 6351 sheet with 1 mm thickness using high-speed steel tool. They have examined the effect of spindle speed, conical angle and feed rate on the outputs of thermal drilling such as axial force and torque. The results of this experiment demonstrated that the thermal drilling at low and medium spindle speed, a high polished surface was found. However, at high spindle speed, discolour surface was observed in the drilled hole.

Somasundaram et al. [16] fabricated the aluminium matrix composite sheets using stir casting process and then it was thermal drilled using high speed steel. In this study, the roundness errors of thermal drilled holes were measured under the different conditions of process parameters such as spindle speed, workpiece thickness, feed rate, and weight percentage of reinforcement particles. They also created a regression model equation for roundness error by using response surface methodology. This study revealed that the roundness error decreased with an increase in the percentage of reinforcement in aluminium matrix composites. However, it was increased with increasing of remaining process parameters.

Table 1
Comprehensive look of previous works in optimization.

Previous works	Material used	Methodology used for optimization	Parameters measured	Inferences
Pantawane et al. [12]	AISI 1015 steel	Taguchi method	surface roughness, axial force, torque	Surface roughness improves when the spindle speed increases, but the axial force and torque decreases
Ku et al. [13]	SUS 304 stainless steel	Taguchi method	Surface roughness, bushing length	Friction angle and spindle speed were the significant parameters that affect surface roughness while friction contact area ratio was the only significant parameter for bushing length
Chow et al. [14]	AISI 304 stainless steel	Taguchi method	Surface roughness	Higher feed rate produced a poor surface finish
Krishna et al. [15]	AA 6351	Taguchi method	Axial force, torque	At high spindle speed, discolour surface was detected in the drilled hole.
Somasundaram et al. [16]	Aluminium metal matrix composite	Response surface methodology	Roundness error	Roundness error decreased with an increase in the percentage of reinforcement in aluminium matrix composites
El-Bahloul et al. [17]	AISI 304 stainless steel	Taguchi Method and Fuzzy Logic	Hole diameter error, roundness error, axial force, radial force, and bushing length	Spindle speed and workpiece thickness are highly influenced the responses characteristics.
Hynes et al. [19]	Galvanized steel	Artificial Neural network and simulated annealing algorithm	Bushing length	Significance of workpiece thickness is very high for getting higher bushing length.
Hynes et al. [23]	Galvanized steel	Artificial Neural network and genetic algorithm	Bushing length	Luders bands were formed inside the bushing length
Bustillo et al. [44]	AISI 1045 steel and Al 5754	Artificial intelligence techniques	Axial force and torque	When the rotational speed is increased, the thrust forces and the torque decrease.

El-Bahloul et al. [17] utilized the Taguchi method and fuzzy logic approach for the optimization of thermal drilling process in AISI 304 stainless steel. They obtained the optimal processing condition by the developed approach. Also, this study confirms that this approach is very simple and competent for multi-objective optimization in this process.

The adaptive neuro fuzzy inference system (ANFIS) is an attractive and powerful soft computing approach which combines two well-established machine learning techniques such as an artificial neural network (ANN) and fuzzy logic theory [18]. The ANFIS approach has the ability to learn from training data just as an ANN and then the solutions mapped out onto a fuzzy inference system (FIS) [19]. Therefore, the hidden layers are determined exactly by a FIS in the network of ANFIS. This eliminates the renowned challenge in the ANN model of determining the hidden layer and together improving its capability of prediction [20]. For that reason, ANFIS is considered since it does not need a complex mathematical model, it is a quick and adaptive approach for developing the prediction model of surface roughness. Previously ANFIS approach has applied to various manufacturing applications such as modeling of surface roughness and cutting zone temperature in dry turning processes [21], modeling of surface roughness in ball end milling process [22].

Genetic algorithm (GA) is a search method used in computing to determine exact or approximate solutions to the problem of optimization [23]. The advantages of GA method are that it has the ability to build explicit models for complex systems and adapt to non-linear equations based on only the data [24]. This model can then be used offline or can be integrated with system for real-time monitoring of system [25,26]. The hybrid approach of GA utilized with ANFIS prolongs its capability of prediction. The proposed approach of ANFIS with GA was already used by the investigators for other applications. Abhishek et al [27] proposed a hybrid technique of ANFIS-GA for predicting axial force and surface roughness in the conventional drilling of glass reinforced polymer composite. The input process parameters used for that developed model were spindle speed, workpiece thickness, drill bit diameter and feed rate which predicted the axial force and surface roughness. Admuthe et al. [28] used this hybrid approach of ANFIS-GA to model and optimize the spinning process parameters in the textile industry. The combined artificial intelligence (AI) techniques such as fuzzy logic and genetic algorithms [29], neural networks and genetic algorithms [30] and fuzzy logic and neural networks [31] are used for prediction and optimization of different problems process parameters. The proposed approach has various advantages such as an ability to capture the nonlinear structure of a process, adaptation ability, fast learning capacity and accurate prediction. Therefore, the hybrid model of ANFIS-GA typically show better performances than the individual technique of AI and display faster adaptation of the structure to the problem. Therefore, the combined ANFIS-GA was utilized in this research work.

The aim of the present work is to examine on a strategy for optimizing machining parameters in the thermal drilling process and the majority of researchers focused on optimization techniques such as Taguchi method, response surface methodology and fuzzy logic technique only. In this study, the combined method of ANFIS and GA has been proposed to optimize the surface roughness of the thermal drilled holes based on the different variables such as spindle speed, tool angle and workpiece thickness. Considering the variables on the surface roughness and finding the optimum state of these variables by the combination of ANFIS and GA for successful thermal drilling in the galvanized steel sheet metal has not been studied yet. To get good surface quality, a well-established predictive model has been required for the manufacturing industry. Therefore, in this present work, a combined ANFIS-GA soft com-

puting technique is established to assess the possibility of prediction and optimization of the surface roughness.

2. Theoretical foundation of surface roughness

After the drilling process, the topography structure of workpiece material is altered at the micro stage. With the purpose of characterizing the parameter of surface roughness in machining areas; the different measures are normally available such as average, root-mean-square and peak-to-valley. However, the most generally used method is the average surface roughness (S) [22]. Fig. 1 shows the general pattern of surface roughness. The parameters such as S_l , S_u , and S_t represent the lower deviation of surface roughness, upper deviation of surface roughness, and total surface roughness.

In any machined part, their surface represents a complex shape made of a series of peaks and troughs of varying heights, depths, and spacing. Surface roughness is defined as the shorter frequency of real surfaces relative to the troughs. The differences in appearance in a product's exterior cover, a vehicle's dashboard or a machined panel, whether something is shiny and smooth or rough, are due to the difference in surface roughness. Appearance and texture can influence a product's added value such as class and customer satisfaction. If a part makes contact with something, its surface roughness affects the amount of wear or the ability to form a seal and the rate of corrosion as well. It has therefore been required in recent years to quantify the asperity of a surface.

Stylus type SJ-210 Mitutoyo instrument is used to measure the surface roughness inside the bushing of thermal-drilled galvanized steel holes. Before that, the specimen is positioned in the fixture. The stylus is allowed to move on a straight line of sampling length 2 mm along the axis of the hole. Surface roughness is calculated as the Roughness Average of a surface measured microscopic peaks and valleys. The average surface roughness is expressed in Eq. (1) [22]

$$S = 1/L \int_0^L |Y(x)dx| \quad (1)$$

where S is the average of peak heights and valleys calculated arithmetically, measured with the sampling length of 2 mm and L represents sampling length.

3. Experimentation

Thermal drilling process conducted on DP 600 grade type galvanized steel material using developed drilling machine along with 0.1–11 kW 3 Phase Variable Frequency Drive. Thermal drilling setup is done by retrofitting the existing drilling setup. The motor power is altered as it requires huge power as compared with the existing drilling process. Since the thermal drilling is a thermo-mechanical process which initially involves an axial force and later the heat generated using the friction is utilized to soften the workpiece to be drilled. The motor of 1.5 HP is fitted into the drilling set up. Belt with the specification of A 1102 V-belt is utilized to transmit the power from the motor shaft to drill assembly. Table 2 shows the three levels of process parameters for experimentation. Spindle speed (N) is varied from 1600 to 2400 rpm, angle of tool is varied from 30 to 45 degree and workpiece thickness is varied from 1 to 2 mm. The feed rate is kept constant at 100 mm/min. Galvanized steel is chosen as workpiece material with the dimension of 150 × 100 mm and thickness of 1, 1.5, and 2 mm. In this investigation, the Taguchi orthogonal array adopted is L27 for three parameter three level conditions and measure output values are shown in Table 3.

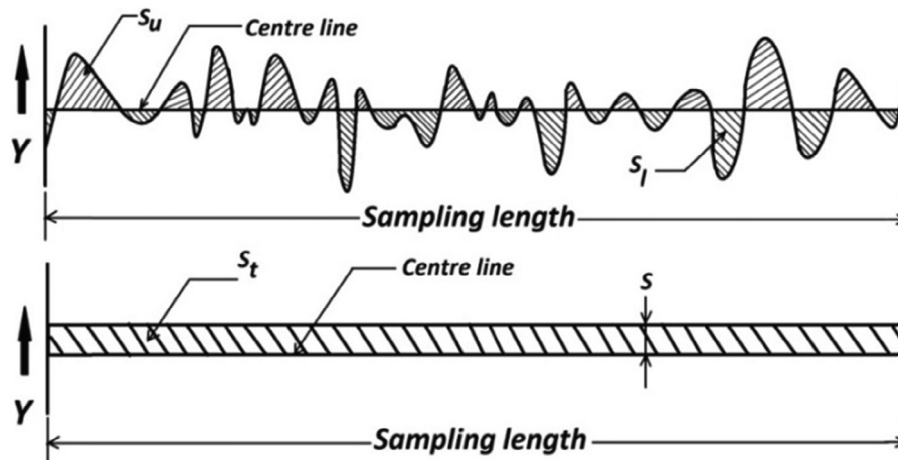


Fig. 1. General pattern of surface roughness [32].

Table 2
Thermal drilling parameters and their levels.

Factors	Symbol	Levels		
		-1	0	+1
Spindle speed (rpm)	N	1600	2000	2400
Angle of tool (degree)	A	30	37.5	45
Workpiece thickness (mm)	H	1	1.5	2

Table 3
Taguchi L27 Orthogonal Array and measured responses.

Run	N	A	H	Surface roughness (μm)
1	-1	-1	-1	2.529
2	-1	-1	0	2.613
3	-1	-1	1	2.686
4	-1	0	-1	2.789
5	-1	0	0	2.863
6	-1	0	1	2.951
7	-1	1	-1	3.029
8	-1	1	0	3.143
9	-1	1	1	3.197
10	0	-1	-1	1.998
11	0	-1	0	2.093
12	0	-1	1	2.106
13	0	0	-1	2.152
14	0	0	0	2.224
15	0	0	1	2.258
16	0	1	-1	2.324
17	0	1	0	2.478
18	0	1	1	2.433
19	1	-1	-1	1.052
20	1	-1	0	1.085
21	1	-1	1	1.156
22	1	0	-1	1.211
23	1	0	0	1.336
24	1	0	1	1.399
25	1	1	-1	1.421
26	1	1	0	1.495
27	1	1	1	1.524

Fig. 2(a) & (b) shows the experimental setup arrangement and samples produced by the thermal drilling process respectively. The average surface roughness (S) for each drilled holes are measured using Mitutoyo SJ-210 Portable Surface Roughness Tester. In this study, the influences of controlled drilling process parameters such as spindle speed, angle of tool and workpiece thickness on surface roughness are studied. Totally, 27 datasets were employed based on experimental design. Eighteen datasets of

experimentation were selected randomly [33] entitled training data (Table 4), for the purposes of the training process of ANFIS model, while the remaining nine datasets, named testing data (Table 5) were assigned to the trained ANFIS model in order to verify the accuracy of prediction of the system.

4. Methodology

4.1. Adaptive neuro-fuzzy inference system (ANFIS)

ANFIS has been effectively applied to classification tasks, rule-based process controls, pattern recognition problems and the function approximation problems [34]. In ANFIS architecture, both artificial neural network and fuzzy logic are combined and the mapping relation between the input and output data defines the optimal distribution of membership functions. It integrates the adaptive neural network (ANN) rules and fuzzy logic (FL) theory inside the adaptive network frameworks. From FL theory, the fuzzy inference system (FIS) application has been derived and the membership functions (MF) in FIS improved through trial and error. In the ANFIS technique, ANN procedure is engaged to develop the FIS model and through which it permits to learn the neural network training data form the given data. At the same time, the results have been mapped by the factors in the arrangement of Sugeno category IF-THEN rules.

The general architecture of the ANFIS structure is shown in Fig. 3. Fundamentally, five different layers are used to create this inference system. They are (i) fuzzy layer, (ii) product layer, (iii) normalized layer, (iv) de-fuzzy layer, and (v) total output layer. Every single layer consists of different nodes in which squares represent the adaptive nodes where the factors could be changed. However, circles represent the fixed nodes, where the factors are fixed.

The inputs of present layers are attained from the nodes in the earlier layers. In order to demonstrate the ANFIS procedures, for simplicity, it is assumed those two inputs (a, b) and one output (S_i) in this system [35]. The ANFIS rule base contains Sugeno type IF-THEN fuzzy rules. For a first order Sugeno-fuzzy inference system (FIS), the two IF-THEN rules may be expressed as follows

$$\text{Rule I} \rightarrow \text{IF } a \text{ is } X_1 \text{ and } b \text{ is } Y_1; \text{ THEN } c \text{ is } S_1(a, b) \quad (2)$$

$$\text{Rule II} \rightarrow \text{IF } a \text{ is } X_2 \text{ and } b \text{ is } Y_2; \text{ THEN } c \text{ is } S_2(a, b) \quad (3)$$

where a and b are the ANFIS inputs, P_i and Q_i represent fuzzy sets. $S_i(a, b)$ is a first order Sugeno- FIS.

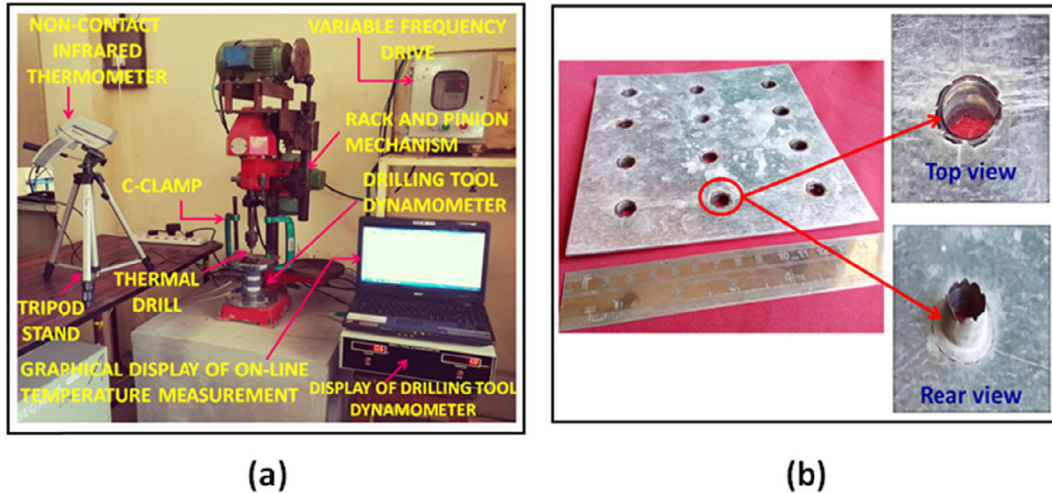


Fig. 2. (a) Experimental setup of the thermal drilling process (b) Samples of thermal drilled holes are produced in galvanized steel.

Table 4
Training datasets for ANFIS model.

Sl. no	Spindle speed (rpm)	Angle of tool (degree)	Workpiece thickness (mm)	Surface roughness (μm)
1	1600	30	1	2.529
2	1600	30	2	2.686
3	1600	37.5	1.5	2.863
4	1600	37.5	2	2.951
5	1600	45	1	3.029
6	1600	45	2	3.197
7	2000	30	1.5	2.093
8	2000	30	2	2.106
9	2000	37.5	1	2.152
10	2000	37.5	2	2.258
11	2000	45	1	2.324
12	2000	45	1.5	2.478
13	2400	30	1	1.052
14	2400	30	1.5	1.085
15	2400	37.5	1	1.211
16	2400	37.5	2	1.399
17	2400	45	1.5	1.495
18	2400	45	2	1.524

Table 5
Testing datasets for ANFIS model.

Sl. no	Spindle speed (rpm)	Angle of tool (degree)	Workpiece thickness (mm)	Surface roughness (μm)
1	1600	30	1.5	2.613
2	1600	37.5	1	2.789
3	1600	45	1.5	3.143
4	2000	30	1	1.998
5	2000	37.5	1.5	2.224
6	2000	45	2	2.433
7	2400	30	2	1.156
8	2400	37.5	1.5	1.336
9	2400	45	1	1.421

4.1.1. Fuzzy layer

The fuzzy layer comprises adaptive nodes with node function. It converts the inputs (a, b) into linguistic labels (X_1, X_2, Y_1 and Y_2) used for separating the membership functions. The output of each node is determined by the Eqs. (4) and (5) [36]

$$O_{1,i} = \mu_{X_i}(a) \quad \text{for } i = 1, 2 \tag{4}$$

$$O_{1,i} = \mu_{Y_{i-2}}(b) \quad \text{for } i = 3, 4 \tag{5}$$

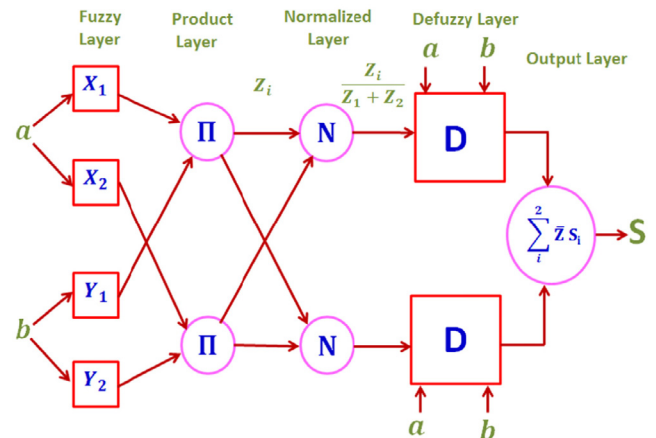


Fig. 3. General ANFIS architecture [36].

where $O_{1,i}$ represents the output function; μ_{X_i} and $\mu_{Y_{i-2}}$ represent the membership functions. Typically, the various membership functions are available such as triangular shaped membership function (trimf), trapezoidal shaped membership function (trapmf), generalized bell shaped membership function (gbellmf), gaussian curve membership function (gaussmf), gaussian combination membership function (gauss2mf), Π -shaped membership function (pimf), difference between two sigmoidal membership functions (dsigmf), product of two sigmoidal membership functions (psigmf).

In trimf, the triangular curve is a function of a vector, a and depends on three scalar parameters p, q , and r as follows [37]

$$\mu_{X_i}(a; p, q, r) = \begin{cases} 0, & a \leq p \\ \frac{a-p}{q-p}, & p \leq a \leq q \\ \frac{r-a}{r-q}, & q \leq a \leq r \\ 0, & r \leq a \end{cases} \tag{6}$$

The parameters p and r locate the feet of the triangle and the parameter q locates the peak as shown in Fig. 4 (a).

In trapmf, the trapezoidal curve is a function of a vector, a and depends on four scalar parameters p, q, r , and s as shown in following expression [37]



Fig. 4. (a) Triangular membership function (b) Trapezoidal membership function.

$$\mu_{X_i}(a; p, q, r, s) = \begin{cases} 0, & a \leq p \\ \frac{a-p}{q-p}, & p \leq a \leq q \\ 1, & q \leq a \leq r \\ \frac{s-a}{s-r}, & r \leq a \leq s \\ 0, & s \leq a \end{cases} \quad (7)$$

The parameters p and s locate the feet of the trapezoid and the parameters q and r locate the shoulders as shown in Fig. 4(b).

In gbellmf, the generalized bell shaped curve is a function of a vector, a , and depends on three parameters p, q , and r are as given by [37]

$$\mu_{X_i}(a; p, q, r) = \frac{1}{1 + \left| \frac{a-r}{p} \right|^{2q}} \quad (8)$$

The parameters p and r locate the feet of the generalized bell shaped curve in which the parameter q is generally positive. The parameter r represents the center of the curve.

In gaussmf and gauss2mf, curves is a function of a vector, a , and depends on two parameters σ and c as shown in following expression [37],

$$\mu_{X_i}(a; \sigma, c) = e^{-\frac{(a-c)^2}{2\sigma^2}} \quad (9)$$

The spline based curve is also known as Π -shaped curve (pimf), it is a function of a vector, a , and depends on four parameters p, q, r , and s as shown in following expression [37],

$$\mu_{X_i}(a; p, q, r, s) = \begin{cases} 0, & a \leq p \\ 2\left(\frac{a-p}{q-r}\right)^2, & p \leq a \leq \frac{p+q}{2} \\ 1 - 2\left(\frac{a-q}{q-r}\right)^2, & \frac{p+q}{2} \leq a \leq q \\ 1, & q \leq a \leq r \\ 1 - 2\left(\frac{a-r}{s-r}\right)^2, & r \leq a \leq \frac{r+s}{2} \\ 2\left(\frac{a-s}{s-r}\right)^2, & \frac{r+s}{2} \leq a \leq s \\ 0, & a \geq s \end{cases} \quad (10)$$

The parameters p and s represent the feet of the curve, while q and r represent its shoulders.

In dsigmf, the difference between two sigmoidal curves is a function of a vector, a , and depends on two parameters p and r as shown in the following expression [37],

$$\mu_{X_i}(a; p, r) = \frac{1}{1 + e^{-p(a-r)}} \quad (11)$$

This dsigmf membership function is the difference between two sigmoidal curves [37],

$$\mu_{X_i}(a; p_1, r_1) - \mu_{X_i}(a; p_2, r_2) \quad (12)$$

In psigmf, the product of two sigmoidal curves is simply the product of two such curves and depends on two parameters p and r [37],

$$\mu_{X_i}(a; p_1, r_1) \times \mu_{X_i}(a; p_2, r_2) \quad (13)$$

4.1.2. Product layer

The fixed nodes are used in this layer and it is marked by a circle and labeled as Π . The output of each node is the product of all the received signals from the previous layer. The following expression shows the output of this layer [38]

$$O_{2,i} = Z_i = \mu_{X_i}(a) \cdot \mu_{Y_i}(b) \quad \text{for } i = 1, 2 \quad (14)$$

The output Z_i of each node denotes the firing strength of a rule.

4.1.3. Normalized layer

Every node in a normalized layer is represented by a fixed node which is marked by a circle and labeled by N . It is defined as the ratio of the i^{th} node firing strength (Z_i) to the sum of all rules firing strengths as shown in Eq. (15) [38]

$$O_{3,i} = \bar{Z} = \frac{Z_i}{Z_1 + Z_2} \quad \text{for } i = 1, 2 \quad (15)$$

where $O_{3,i}$ and \bar{Z} denote the output of the normalized layer and normalized firing strength respectively. The output of the normalized layer and normalized firing strength is only acceptable within a range of 0 to 1.

4.1.4. Defuzzy layer

The fourth layer is the defuzzification layer which consists of adaptive nature nodes and it is marked by the square and labeled by D . It computes the multiplication of normalized firing strength and first order polynomial. Therefore, the output of this defuzzy layer is specified by the expression [38]

$$O_{4,i} = \bar{Z} \cdot S_i = \bar{Z} (e_i a + f_i b + g_i) \quad \text{for } i = 1, 2 \quad (16)$$

where e_i, f_i and g_i are the consequent parameters.

4.1.5. Output layer

The fifth layer is the output layer which has one fixed node, marked by a circle. Here the node function is to compute the overall output as given in the following equation [38]

$$O_{5,i} = \sum_i^2 \bar{Z} S_i = \sum_i^2 \bar{Z} (e_i a + f_i b + g_i) \\ = \text{Overall output for } i = 1, 2 \quad (17)$$

To increase the convergence rate, an algorithm used for this present work is a hybrid learning algorithm. This algorithm is used to integrate the least square and gradient descent method in order to update the premise parameters. The least square method is utilized to optimize the consequent parameters. After getting the optimal consequent parameters, the gradient descent method is employed to regulate optimally the premise parameters. The output of ANFIS is determined by using consequent parameters. The total output is given by the following equation [38],

$$\text{Total output} = \bar{Z} S_1 + \bar{Z} S_2 = \frac{Z_1}{Z_1 + Z_2} S_1 + \frac{Z_2}{Z_1 + Z_2} S_2 \\ = \frac{Z_1}{Z_1 + Z_2} (e_1 F_1 + f_1 F_2 + g_1) \\ + \frac{Z_2}{Z_1 + Z_2} (e_2 F_1 + f_2 F_2 + g_2) \quad (18)$$

4.2. Genetic algorithm

Genetic algorithm (GA) is a recognized technique to optimize an objective function along with linear or non-linear boundaries. GA is a stochastic global searching technique based on the principles of natural selection and genetics in which the error function derivative assessment is not necessary. Also, it is a well-organized to be tremendously efficient in dealing with non-linear as well as poor complex optimization problems [39]. Nowadays, GA is one of the most attractive techniques for optimization of problems in the various fields of industrial application since it has robustness in determining an optimal solution which is the nearly global minimum. GA activates according to the principle of survival of the fitness on a population of potential solutions to create better approximations towards a solution. At each solution generation, new approximations set is produced by the procedure of selecting individuals based on the fitness level in the domain of the problem. This practice leads to the growth of well-suited populations. A candidate solution in GA technique is represented by means of genes sequence which is called chromosome. The chromosome potential is named its fitness function, which is assessed through objective function. Population means a set of selected chromosomes which is subjected to the number of iterations (generations). For each generation, a new population is created by the operators of GA such as selection, crossover, and mutation. Greatly fitness individuals are given chances to replicate through exchanging of their genetic statistics. This creates a new offspring solution, which would share the good characteristics acquired from parents. Mutation operation is employed subsequently crossover by shifting certain genes in the strings. The offspring can either replace a smaller amount of fitness individuals or replace the whole population. This assessment and selection of reproduction sequence are continuously performed until an acceptable solution is obtained.

5. Results and discussion

5.1. Prediction of surface roughness by ANFIS

The ANFIS structure and network model are used for this work to predict surface roughness of the thermal drilled hole which is shown in Fig. 5(a) & (b). It performs the systems of Sugeno type FIS and membership function are employed to do the training process. In this work, the FIS considers the three inputs of thermal drilling parameters like spindle speed (N), angle of tool (A) and workpiece thickness (H).

Grid partition technique is used to generate the optimized rules of a given dataset. The dataset in Table 4 is employed to train the ANFIS model and the predictive competence of the corresponding model is tested on the dataset in Table 5. Fig. 6 shows the loading of training data into the ANFIS model.

The ANFIS model has performed the training process on the training dataset and finally test the results with testing data. While the training process of the ANFIS model, the input dataset is plotted several times to reduce the prediction error. The required number of iterations in order to mapping is stated as epochs. From Fig. 6 it is noticed the 100 epochs (no. of iterations) are essential to accomplishing the training process on 18 datasets. Fig. 7 shows the loading of testing data into the ANFIS model. It can be seen from Fig. 7 after the training process, and then it is tested on 9 datasets, with the aim of validation of the model.

Table 6 displays the results of the training and testing process of the ANFIS model with the different type of membership functions. From the results in Table 6, gbell membership function in comparison with the other membership functions which have low prediction error i.e. RMSE for training is 2.4418×10^{-6} and for testing is 1.8533. It can result that the best optimal ANFIS structure with 3 3 3 membership function for this process. Fig. 8 shows the training error curve for the experimental values of thermal drilled workpiece surface roughness. Fig. 9 shows experimental outcomes of surface roughness under the same processing conditions as the training and testing datasets are utilized to compare the predicted surface roughness results by the ANFIS model.

5.2. Optimization of surface roughness by GA

Generally, a requirement of optimization for solving several manufacturing problems in which surface roughness (S) function has to be minimized. Table 7 shows the setting parameters in GA toolbox. Initially, the optimization problem of surface roughness in the thermal drilling of galvanized steel should be defined in terms of a mathematical model equation or fitness function. This equation is given as the functional dependence of measured value and the drilling parameters [40]. Due to the complexity of models, more accurate mathematical models contain linear and non-linear components. But in actual practice, second-order polynomials are sufficient to develop a mathematical model for the description of the manufacturing process.

This research work was performed with the three input (independent) variables such as rotational speed (N), angle of tool (A) and workpiece thickness (H). In order to determine a suitable parameter range, preliminary tests were conducted effectively. The spindle speed (N) was varied between 1600 rpm and 2400 rpm, angle of tool (A) was varied between 30 degree to 45 degree, workpiece thickness (H) was varied between 1 mm and 2 mm. The influence over the surface roughness of thermal drilling parameters was determined based on the experimental results using the equation given below:

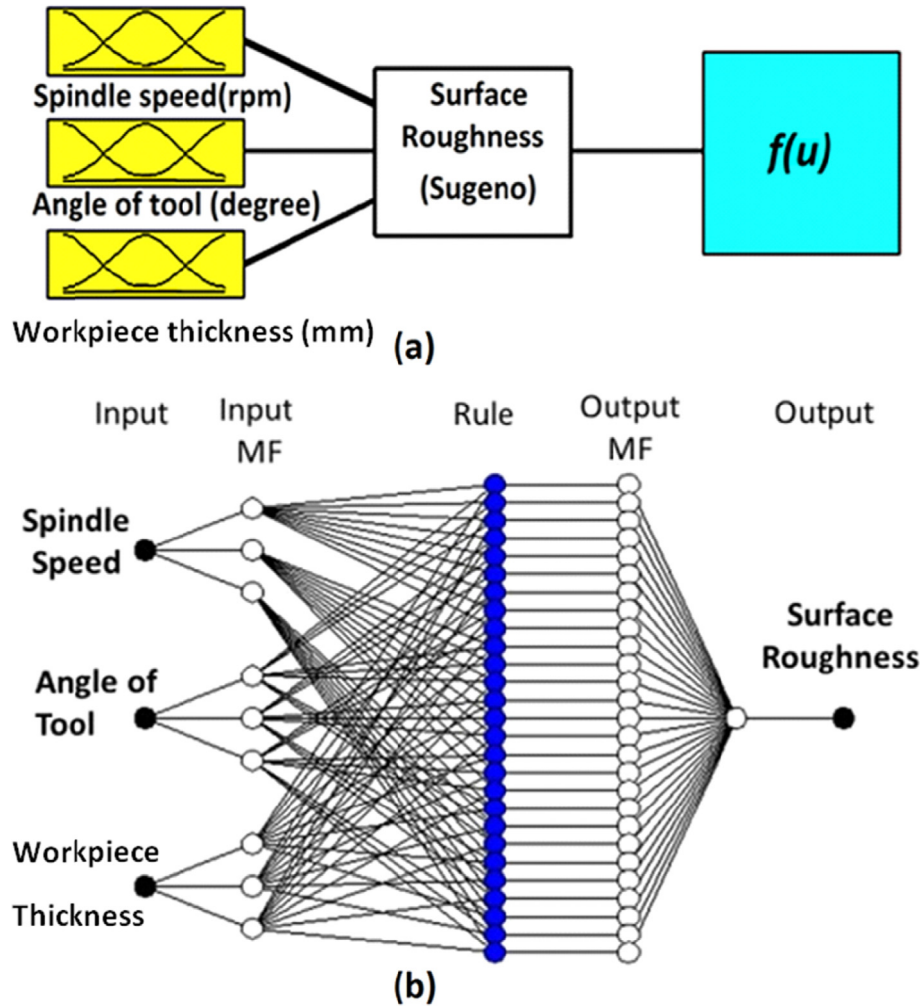


Fig. 5. Developed ANFIS structure and (b) neural network model for surface roughness.

$$\begin{aligned}
 \text{Surface roughness}(S) = & 0.0593796 + 0.00217889 \times N \\
 & + 0.0511963 \times A + 0.521389 \times H \\
 & - 9.31597 \times 10^{-7} \times N^2 \\
 & - 3.35802 \times 10^{-5} \times A^2 \\
 & - 0.105556 \times H^2 - 1.01111 \times 10^{-5} \\
 & \times N \times A - 2.58333 \times 10^{-5} \times N \times H \\
 & - 4.22222 \times 10^{-4} \times A \times H \quad (19)
 \end{aligned}$$

Selection of optimal thermal drilling parameters should enhance not only the economical utilization of drilling machine but also the quality of the product to become a better appearance by reducing the value of surface roughness. A fitness function (Eq. (19)) to be minimized is essential to describe the standard optimization problem [41]. In thermal drilling process, the optimization problem can be stated in the following:

Minimize: $S(N, A, H)$
 $S(\text{model}) \leq S(\text{min}) (\mu\text{m})$

Within ranges of thermal drilling process parameters:

Spindle speed: $1600 \text{ rpm} \leq N \leq 2400 \text{ rpm}$

Angle of tool: $30 \text{ degree} \leq A \leq 45 \text{ degree}$

Workpiece thickness: $1 \text{ mm} \leq H \leq 3 \text{ mm}$

The GA toolbox of MATLAB R2010a software used to determine the minimum of the fitness function [42]. This function could be expressed in the MATLAB file (M-file) and permits it is an argument to the main GA function. The M-file used for optimization in GA toolbox that computes the fitness function must proceed a row vector 'y' of length 3, corresponding to the independent variables y_1 , y_2 and y_3 , and return a scalar equivalent to the value of the function at y. The M-file can be expressed as follows:

function z = surface_roughness(y)

$$\begin{aligned}
 z = & 0.0593796 + 0.00217889 \times y(1) + 0.0511963 \times y(2) \\
 & + 0.521389 \times y(3) - 9.31597 \times 10^{-7} \times (y(1))^2 \\
 & - 3.35802 \times 10^{-5} \times (y(2))^2 - 0.105556 \times (y(3))^2 \\
 & - 1.01111 \times 10^{-5} \times y(1) \times y(2) - 2.58333 \times 10^{-5} \times y(1) \\
 & \times y(3) - 4.22222 \times 10^{-4} \times y(2) \times y(3) \quad (20)
 \end{aligned}$$

Then, save the M-file of Eq. (20) in a directory on the path of MATLAB [42]. The population type (double vector) states the input data type to the fitness function. The size of the population (1 0 0) defines how many individuals are there in each generation.

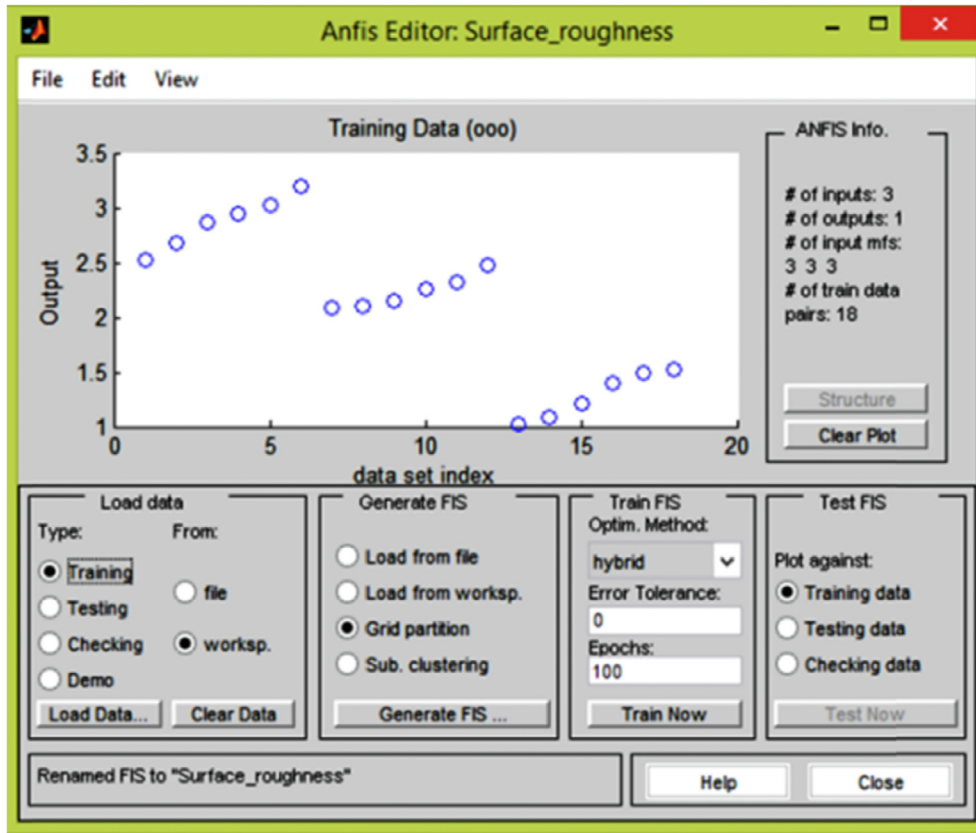


Fig. 6. Initial loading of training dataset.

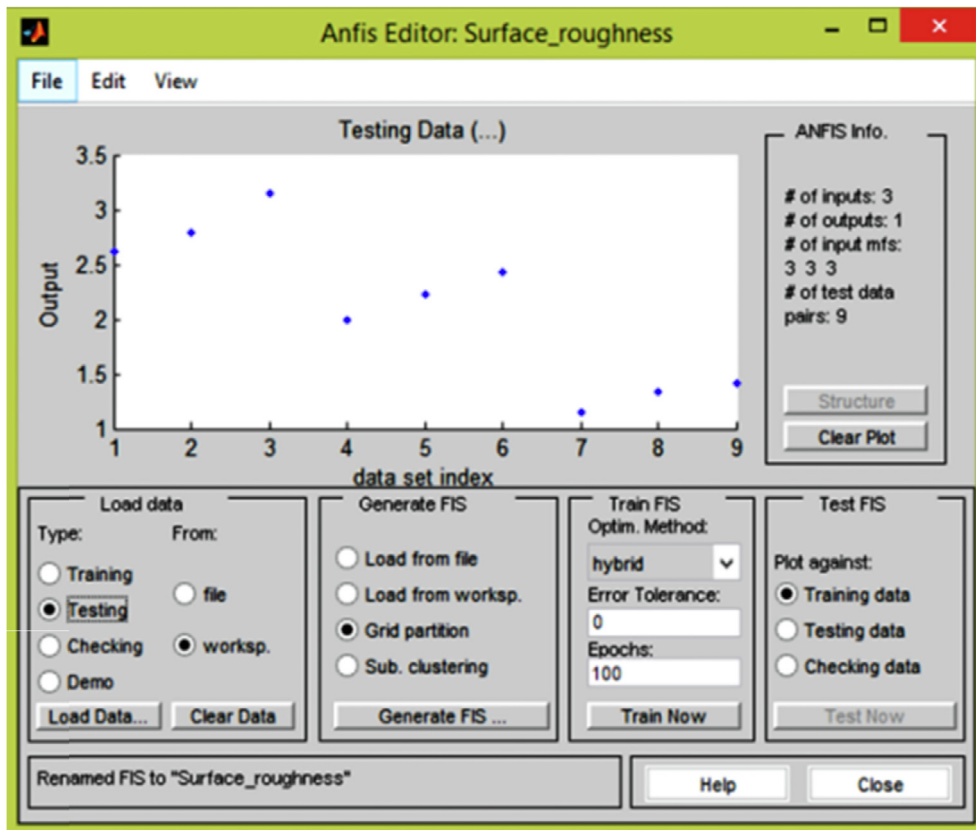


Fig. 7. Initial loading of testing dataset.

Table 6
Comparing of the result of different membership functions.

Sl. no	No. of Membership function	Function type	Output Function	Error (RMSE)	
				Training Error	Testing Error
1	3 3 3	trimf	Constant	2.88500×10^{-6}	4.2124
2			Linear	4.36780×10^{-4}	4.1537
3		trapmf	Constant	2.83860×10^{-6}	2.2232
4			Linear	4.36780×10^{-4}	2.8253
5		gbellmf	Constant	2.44180×10^{-6}	1.8533
6			Linear	1.70290×10^{-3}	3.2931
7		gaussmf	Constant	2.47330×10^{-6}	3.8251
8			Linear	1.86600×10^{-3}	3.2597
9		gauss2mf	Constant	2.53980×10^{-6}	2.2208
10			Linear	1.51280×10^{-3}	2.2199
11		Pimf	Constant	2.63860×10^{-6}	2.4122
12			Linear	4.36780×10^{-4}	2.6832
13		dsigmf	Constant	2.53910×10^{-6}	2.1957
14			Linear	1.73630×10^{-3}	2.2142
15		psigmf	Constant	2.83770×10^{-6}	2.1004
16			Linear	1.64030×10^{-3}	2.2134

According to the size of the population, the GA has to search point which leads to obtaining a required result. While population size is increasing, causes the GA to execute more slowly.

Based on their scaled values from the fitness function, the selection function selects parents for the next level generation. The present work selects stochastic uniform [43] as a selection function, in which each parent corresponds to a section of the line of length proportional to its scaled value. GA moves along the line in steps of same equal size. At every step, the GA assigns a parent from the section it lands on. The recommendation is to apply different seed numbers for the same parameters to reach results that are more refined. As for crossover rate, it is recommended use a guiding value from 0.7 to 0.9. meanwhile, as for mutation rate it was noticed that reaching optimal solution could occur using both ascending or descending mutation techniques depending on population diversity as it is noticed that increasing the diversity of population along with using a suitable fitness scaling technique that does not allow a gene to dominate the population is best, while in case of decreasing mutation rate it is advised to use a fitness scaling scale that identifies the small differences between individuals. In crossover functions, It is clearly advised that when using a real representation to use crossover function that is based on such representation such as (e.g., arithmetic, heuristic) to obtain optimal values in the least number of evaluations. The crossover fraction and mutation probability of 0.8 and 0.2 specify the population fraction of crossover children and mutation children respectively.

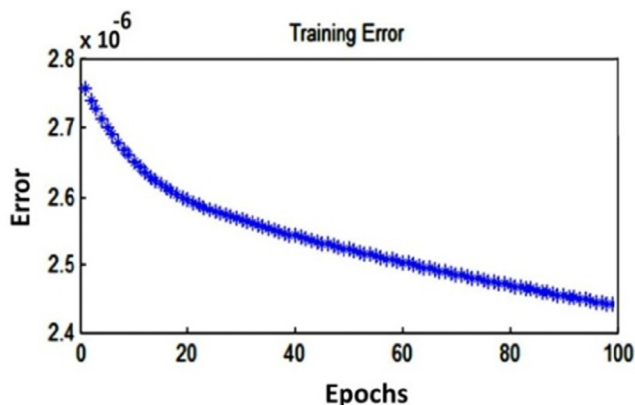


Fig. 8. Training error curve of ANFIS model for surface roughness.

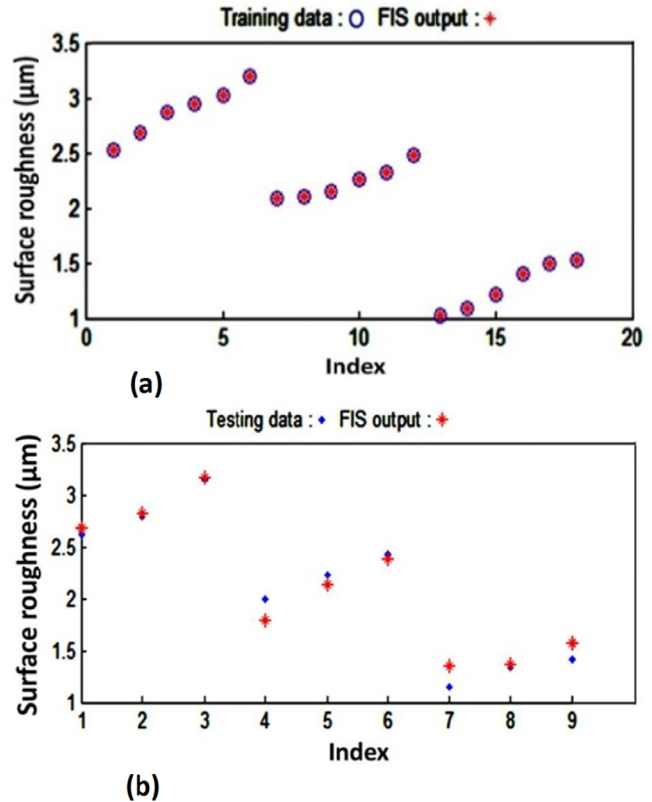


Fig. 9. Comparison of Experimental and Predicted Values (a) training process (b) testing process.

Choice of 0.8 crossover fraction represents the offspring thus formed from 0.8 of the parent 1 and 0.2 of the parent 2. The algorithm creates crossover children by combining pairs of parents in the current population. At each coordinate of the child vector, the default crossover function randomly selects an entry, or gene, at the same coordinate from one of the two parents and assigns it to the child. For problems with linear constraints, the default crossover function creates the child as a random weighted average of the parents. The number of generations denotes the stopping of GA when it reaches the defined value of 100. Also, the stall generations denote stopping of GA if there is no improvement in the fitness function for a sequence of consecutive generations to a defined value of 50. In order to achieve a better result from GA, a trial and error method has been executed by altering the options in GA toolbox of MATLAB software [43]. In this study, an attempt has been made to determine the process parameters for thermal drilling of galvanized steel to minimize the surface roughness with the three different processing conditions using GA. The optimization technique of GA solved the Eq. (20) gives the minimum surface roughness. The values determined by this equation have completely matched with the experimental values. The assessment of generations and the best fitness values found by GA are shown in

Table 7
GA parameters.

Parameters	Values
Number of variables	3
Size of population size	100
Selection function	Stochastic uniform
crossover fraction	0.8
Mutation probability	0.2
Number of generations	100
Stall generations	50

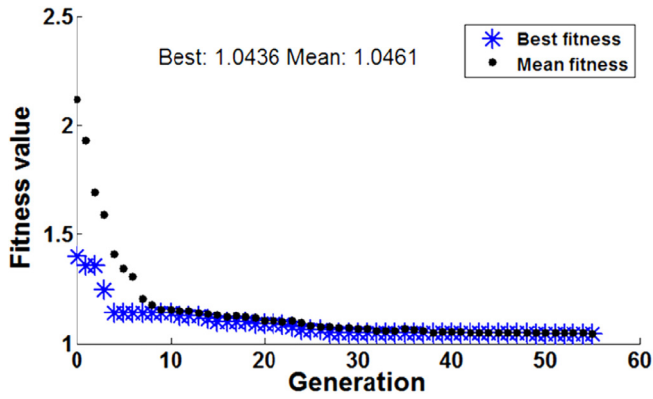


Fig. 10. Fitness plot for surface roughness from genetic algorithm.

Fig. 10. Table 8 shows the comparison of optimized values with the experimental values. The optimized value of surface roughness is obtained from the GA shows a minimum error (0.765%) with the experimental values.

5.3. Effect of thermal drilling input process parameters

Fig. 11(a) shows the surface plot of surface roughness of drilled samples values at the different spindle speeds and workpiece thickness. When spindle speed increased from 1600 to 2400 rpm,

the amount of heat energy is increased steeply to a high speed friction between drill and part. The high heat energy would make the galvanized steel softer and increase the drilling capability. Thus, the better surface quality of a drilled hole was obtained and it was similar to the previous studies of Ku et al. [13] and Chow et al. [14]. However, the surface roughness increases to some extent with the increasing of workpiece thickness from 1 to 2 mm. It is resulted due to increasing of drilling depth. It is observed from Fig. 11(b) & (c) while increasing the angle of tool gradually from 30 to 45 degree, a reduction in contact friction at the interface is obtained and therefore non-uniform temperature distribution would be generated during the performance of thermal drilling process. As a consequence, the starched marks have produced on the surface of the hole during the piercing of workpiece and enhances with the increase in angle of tool additionally. Hence, the higher surface roughness would be formed on the surface of the drilled hole.

6. Conclusions

Thermal drilling process is used to produce a bushing hole from the material of galvanized steel sheet metal that it turns to contribute a supporting portion for producing a number of threads. Galvanized steel is used in the areas of automobile and aerospace engineering. Surface roughness is the predominant output characteristics in the thermal drilling process when compared to others.

Table 8 Comparison of experimental and predicted value of surface roughness.

Process parameters			Surface roughness (μm)	
Spindle speed (rpm)	Angle of tool (degree)	Workpiece thickness (mm)	Experimental values	Optimized value by GA
2400	30	1	1.052	1.0436

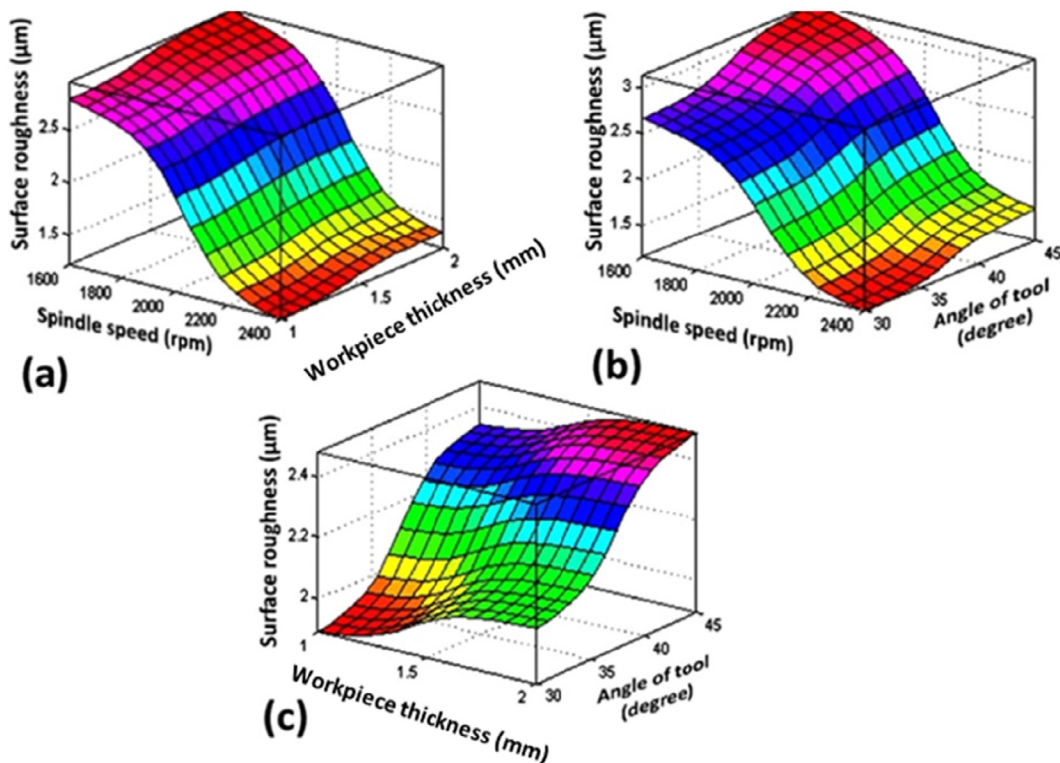


Fig. 11. 3D Surface plots of surface roughness as a function of input parameters.

The proposed ANFIS-GA approach has implemented for prediction and optimization of surface roughness in the drilled holes.

1. The ANFIS model has been attempted for predicting surface roughness of drilled galvanized steel and to find out the optimum parametric setting using the GA method. The thermal drilling parameters were utilized as inputs to the ANFIS model to predict surface roughness. The essential training and testing datasets have been acquired from the experimentation of thermal drilling process. An ANFIS model with gbellmf membership function is selected based on the minimum RSME prediction error of about 2.44180×10^{-6} . It is found that the ANFIS method can be able to attain a better prediction model of the experimental values.
2. An ANFIS based regression model of surface roughness was utilized as a fitness function for GA and after tuning the various parameters, the optimal processing conditions of 2400 rpm spindle speed, 30 degree angle of tool and 1 mm workpiece thickness are obtained. A better correlation of 99.235% is achieved between the predicted and experimental values of surface roughness.
3. From the experimental work, it is concluded that the spindle speed and angle of tool have a greater influence on surface roughness for galvanized steel than the influence of workpiece thickness.

Conflict of interest

The authors have no conflicts of interest to declare.

References

- [1] Z. Demir, C. Özek, M. Bal, An experimental investigation on bushing geometrical properties and density in thermal frictional drilling, *App. Sci.* 8 (2018) 1–10.
- [2] E. Oezkaya, S. Hannich, D. Biermann, Development of a three-dimensional finite element method simulation model to predict modified flow drilling tool performance, *Int. J. Mater. Form.* 1–14 (2018).
- [3] R. Kumar, N.R.J. Hynes, Finite-element simulation and validation of material flow in thermal drilling process, *J. Braz. Soc. Mech. Sci. Eng.* 40 (2018) 1–10.
- [4] N.R.J. Hynes, R. Kumar, Simulation on friction drilling process of Cu₂C, *Mater. Today Proc.* 5 (2018) 27161–27165.
- [5] N.R.J. Hynes, R. Kumar, Simulation and experimental validation of Al7075-T651 Flow Drilling Process, *J. Chin. Soc. Mech. Eng.* 38 (2017) 413–420.
- [6] R. Kumar, N.R.J. Hynes, Influence of rotational speed on mechanical features of thermally drilled holes in dual-phase steel, *P. I. Mech. Eng. B-J. Eng. Manu.* (2018) 1–12.
- [7] U. Caydas, A. Hascalik, O. Buytoz, A. Meyveci, Performance evaluation of different twist drills in dry drilling of AISI 304 austenitic stainless steel, *Mater. Manuf. Process.* 26 (2011) 951–960.
- [8] S.F. Miller, P.J. Blau, A.J. Shih, Tool wear in friction drilling, *Int. J. Mach. Tool. Manuf.* 47 (2007) 1636–1645.
- [9] L. Ozler, N. Dogru, An experimental investigation of hole geometry in friction drilling, *Mater. Manuf. Process.* 28 (2013) 470–475.
- [10] S.F. Miller, J. Tao, A.J. Shih, Friction drilling of cast metals, *Int. J. Mach. Tool. Manuf.* 46 (2006) 1526–1535.
- [11] M.B. Bilgin, K. Gok, A. Gok, Three-dimensional finite element model of friction drilling process in hot forming processes, *P. I. Mech. Eng. E-J. Pro. Mech. Eng.* 231 (2017) 548–554.
- [12] P.D. Pantawane, B.B. Ahuja, Parametric analysis and modelling of friction drilling process on AISI 1015, *Int. J. Mecha. Manuf. Sys.* 7 (2014) 60–79.
- [13] W.L. Ku, C.L. Hung, S.M. Lee, H.M. Chow, Optimization in thermal friction drilling for SUS 304 stainless steel, *Int. J. Adv. Manuf. Tech.* 53 (2011) 935–944.
- [14] H.M. Chow, S.M. Lee, L.D. Yang, Machining characteristic study of friction drilling on AISI304 stainless steel, *J. Mater. Proc. Tech.* 207 (2008) 180–186.
- [15] P.V.G. Krishna, K. Kishore, V.V. Satyanarayana, Some investigations in friction drilling AA6351 using high speed steel tools, *ARNP J. Eng. Appl. Sci.* 5 (2010) 11–15.
- [16] G. Somasundaram, S.R. Boopathy, K. Palanikumar, Modeling and analysis of roundness error in friction drilling of aluminum silicon carbide metal matrix composite, *J. Comp. Mater.* 46 (2011) 169–181.
- [17] S.A. El-Bahloul, H.E. El-Shourbagy, T.T. El-Midany, Optimization of thermal friction drilling process based on Taguchi method and fuzzy logic technique, *Int. J. Sci. Eng. App.* 4 (2015) 55–59.
- [18] J.S.R. Jang, ANFIS: adaptive-network-based fuzzy inference system, *IEEE Trans. Syst. Man Cybern.* 23 (1993) 665–685.
- [19] N.R.J. Hynes, R. Kumar, Process optimization for maximizing bushing length in thermal drilling using integrated ANN-SA approach, *J. Braz. Soc. Mech. Sci. Eng.* 39 (2017) 5097–5108.
- [20] P. Melin, J. Soto, O. Castillo, J. Soria, A new approach for time series prediction using ensembles of ANFIS models, *Expert Syst. Appl.* 39 (2012) 3494–3506.
- [21] M. Aydin, C. Karakuzu, M. Uçar, A. Cengiz, M.A. Çavuşlu, Prediction of surface roughness and cutting zone temperature in dry turning processes of AISI304 stainless steel using ANFIS with PSO learning, *Int. J. Adv. Manuf. Technol.* 67 (2013) 957–967.
- [22] S.J. Hossain, N. Ahmad, Adaptive neuro-fuzzy inference system (ANFIS) based surface roughness prediction model for ball end milling operation, *J. Mech. Eng. Res.* 4 (2012) 112–129.
- [23] N.R.J. Hynes, R. Kumar, J.A.J. Angela, Optimum bushing length in thermal drilling of galvanized steel using artificial neural network coupled with genetic algorithm, *Mater. Tech.* 38 (2017) 413–420.
- [24] A. Garg, K. Shankhwar, D. Jiang, V. Vijayaraghavan, B.N. Panda, S.S. Panda, An evolutionary framework in modelling of multi-output characteristics of the bone drilling process, *Neural Comput. Appl.* 29 (2018) 1233–1241.
- [25] A. Garg, V. Vijayaraghavan, J. Zhang, J.S.L. Lam, Robust model design for evaluation of power characteristics of the cleaner energy system, *Renew. Energ.* 112 (2017) 302–313.
- [26] Y. Huang, L. Gao, Z. Yi, K. Tai, P. Kalita, P. Prapainainar, A. Garg, An application of evolutionary system identification algorithm in modelling of energy production system, *Meas.* 114 (2018) 122–131.
- [27] K. Abhishek, B.N. Panda, S. Datta, S.S. Mahapatra, Comparing predictability of genetic programming and ANFIS on drilling performance modeling for GFRP composites, *Proc. Mater. Sci.* 6 (2014) 544–550.
- [28] L.S. Admuthe, S.D. Apte, Computational model using ANFIS and GA: application for textile spinning process, *IEEE Xplore* (2009) 110–114.
- [29] W.H. Ho, J.T. Tsai, B.T. Lin, J.H. Chen, Adaptive network - based fuzzy inference system for prediction of surface roughness in end milling process using hybrid Taguchi-genetic learning algorithm, *Expert Syst. Appl.* 36 (2009) 3216–3222.
- [30] I.N. Tansel, B. Ozcelik, W.Y. Bao, P. Chen, D. Rincon, S.Y. Yang, A. Yenilmez, Selection of optimal cutting conditions by using GONNS, *Int. J. Mach. Tool. Manuf.* 46 (2006) 26–35.
- [31] R.K. Jain, V.K. Jain, Optimum selection of machining conditions in abrasive flow machining using neural network, *J. Mater. Proc. Tech.* 108 (2000) 62–67.
- [32] M. Jurevicius, J. Skeivalas, R. Urbanavicius, Analysis of surface roughness parameters digital image identification, *Meas.* 56 (2014) 81–87.
- [33] A. Yaghoobi, M.B. Jooybari, A. Gorji, H. Baseri, Application of adaptive neuro fuzzy inference system and genetic algorithm for pressure path optimization in sheet hydroforming process, *Int. J. Adv. Manuf. Technol.* 86 (2016) 2667–2677.
- [34] N.T.S. Bakinde, N. Faruk, S.I. Popoola, M.A. Salman, A.A. Oloyede, L.A. Olawoyin, C.T. Calafate, Path loss predictions for multi-transmitter radio propagation in VHF bands using Adaptive Neuro-Fuzzy Inference System, *Eng. Sci. Technol. Int. J.* 21 (2018) 679–691.
- [35] R.N. Mishra, K.B. Mohanty, Real time implementation of an ANFIS-based induction motor drive via feedback linearization for performance enhancement, *Eng. Sci. Technol. Int. J.* 19 (2016) 1714–1730.
- [36] N. Mathur, I. Glesk, A. Buis, Comparison of adaptive neuro-fuzzy inference system (ANFIS) and Gaussian processes for machine learning (GPML) algorithms for the prediction of skin temperature in lower limb prostheses, *Med. Eng. Phys.* 38 (2016) 1083–1089.
- [37] G.A. Bhosale, R.V. Kulkarni, Performance evaluation using selected fuzzy membership function, *Int. J. Inform. Sys.* 5 (2014) 33–37.
- [38] İ. Asiltürk, M. Tinkir, H.E. Monuayri, L. Çelik, An intelligent system approach for surface roughness and vibrations prediction in cylindrical grinding, *Int. J. Comput. Integ. M.* 25 (2012) 750–759.
- [39] J.S. Trivedi, S. Nair, C. Iyunnai, Optimum utilization of fly ash for stabilization of sub-grade soil using genetic algorithm, *Proc. Eng.* 51 (2013) 250–258.
- [40] V. Savas, C. Ozyay, The optimization of the surface roughness in the process of tangential turn-milling using genetic algorithm, *Int. J. Adv. Manuf. Tech.* 37 (2008) 335–340.
- [41] N. Sharma, R. Khanna, R.D. Gupta, WEDM process variables investigation for HSLA by response surface methodology and genetic algorithm, *Eng. Sci. Technol. Int. J.* 18 (2015) 171–177.
- [42] M.P. Satpathy, B.R. Moharana, S. Dewangan, S.K. Sahoo, Modeling and optimization of ultrasonic metal welding on dissimilar sheets using fuzzy based genetic algorithm approach, *Eng. Sci. Technol. Int. J.* 18 (2015) 634–647.
- [43] S. Kumar, M. Gupta, P.S. Satsang, Multiple-response optimization of cutting forces in turning of UD-GFRP composite using Distance-Based Pareto Genetic Algorithm approach, *Eng. Sci. Technol. Int. J.* 18 (2015) 680–695.
- [44] A. Bustillo, G. Urbikain, J.M. Perez, O.M. Pereira, L.N.L. de Lacalle, Smart optimization of a friction-drilling process based on boosting ensembles, *J. Manuf. Sys.* 48 (2018) 108–121.